Title:

Investigation on the effects of pilot injection on low temperature combustion in high-speed diesel engine fueled with *n*-butanol-diesel blends

Author names and affiliations:

Haozhong Huang[1,*], Qingsheng Liu[1], Ruzhi Yang[1], Tianru Zhu[1], Ruiqing Zhao[1] Yaodong Wang [2]

1. College of Mechanical Engineering, Guangxi University, Nanning 530004, China

2. Sir Joseph Swan Institute for Energy Research, Newcastle University, Newcastle Upon Tyne, NE1 7RU, UK

Corresponding author:

Haozhong Huang, College of Mechanical Engineering, Guangxi University, P.R.China, Daxuedong Road 100, Xixiangtang District, Nanning , China, 530004, Tel./Fax: +86 771 3232294. E-mail: hhz421@gxu.edu.cn (H. Huang).

Abstract

The effect of pilot injection timing and pilot injection mass on combustion and emission characteristics under medium exhaust gas recirculation (EGR (25%)) condition were experimentally investigated in high-speed diesel engine. Diesel fuel (B0), two blends of butanol and diesel fuel denoted as B20 (20% butanol and 80% diesel in volume), and B30 (30% butanol and 70% diesel in volume) were tested. The results show that, for all fuels, when advancing the pilot injection timing, the peak value of heat release rate decreases for pre-injection fuel, but increases slightly for the main-injection fuel. Moreover, the in-cylinder pressure peak value reduces with the rise of maximum pressure rise rate (MPRR), while NO_x and soot emissions reduce. Increasing the pilot injection fuel mass, the peak value of heat release rate for pre-injected fuel increases, but for the main-injection, the peak descends, and the in-cylinder pressure peak value and NO_x emissions increase, while soot emission decreases at first and then increases. Blending *n*-butanol in diesel improves soot emissions. When pilot injection is adopted, the increase of *n*-butanol ratio causes the MPRR increasing and the crank angle location for 50% cumulative heat release (CA50) advancing, as well as NO_x and soot emissions decreasing. The simulation of the combustion of *n*-butanol-diesel fuel blends, which was based on the *n*-heptane-*n*-butanol-PAH-toluene mixing mechanism, demonstrated that the addition of *n*-butanol consumed OH free radicals was able to delay the ignition time.

Keywords: n-butanol-diesel blends, pilot injection, kinetic simulation, Engine performance, Exhaust emission

1. Introduction

The high compression ratio and inherent lean burn of diesel engines allow for highest thermal efficiency, enabling heat dissipation by the excess air. However, diesel engines produce diesel exhaust that contains fine and harmful particles; nowadays researches aim to achieve the highest efficiency and lowest emissions.

For traditional combustion, a reciprocal relationship between NO_x and PM (soot) emissions is established, thus the higher the emissions of NO_x, the lower the PM emissions, and vice-versa. To reduce both, controlling the combustion temperature of the fuel in the engine cylinder (low temperature combustion), is considered as a promising method. The effects of low temperature combustion on diesel engine performance, combustion, and emissions have been deeply investigated [1-4].

In recent years, the energy consumptions and the depletion of fossil fuels including petroleum are increasing rapidly and the need of an alternative suitable fuel for traditional internal combustion engines is being felt. *N*-butanol is regarded as one of the most representative of green substitute fuels [5 – 7] and its use was investigated in different engines [8 – 10]. Compared with methanol and ethanol, *n*-butanol is more soluble in diesel fuel, does not corrode carbon steel and is hydrophilic. Moreover, *n*-butanol has higher gross calorific value, higher carbon content and higher cetane number, lower evaporating pressure and auto-ignition temperature, it is easy to evaporate, has a wider range of air-fuel ratio, higher flashing point, and it is accessible for current fuel transportation equipment with higher security [11-14]. In addition, as oxygenated fuel, blending n-butanol to diesel could bring in more oxygen in fuel-enriched area, and the oxygen atom could react with the soot precursor to reduce the soot emission [15]. Valentino et al. [16] studied the influence of inlet oxygen concentration on combustion and emission performances of *n*-butanol/diesel fuel blends in low temperature combustion, conducting tests at constant speed and constant load. The results showed that soot emissions reduce

58 with the increase of the inlet oxygen concentration.

59 Although many researchers [17-22] investigated engine performance and exhaust emissions in
60 diesel engines fueled with diesel-n-butanol blends, only a few papers focus on the use of such blends at
61 low temperature combustion and on the effects on engine performance and exhaust emissions. Zheng et
62 al. [23] experimentally investigated the effect of two-stage injection on combustion and emissions
63 under high exhaust gas recirculation (EGR) rate on a diesel engine fueled with *n*-butanol/diesel fuel
64 blend. Results show that blending *n*-butanol in diesel improves smoke emissions while induces
65 increase in maximum pressure rise rate (MPRR).

66 The fuel injection system remarkably influences combustion and emissions of diesel engines.
67 High-pressure common rail injection system can affect the spray characteristics and combustion
68 process by controlling the injection quality, injection pressure, and injection timing precisely and
69 flexibly. A multiple injection system is regarded as a vital solution to reduce NO_x and soot emissions
70 simultaneously [24-28]. Pilot injection can improve the combustion and emission performance by
71 adequate pilot injection fuel mass and timing. Thurnheer [29] conducted his research at constant speed,
72 load, EGR ratio, and air-fuel ratio to study the effect of pilot injection timing and pilot-injection fuel
73 mass on combustion and emissions of a heavy diesel engine. The results reveal that advancing pilot
74 injection timing, the combustion starting point advances and pilot injection delay prolongs. Moreover,
75 timing and mass of pilot injection have a little influence on heat release peak in main-injection, and the
76 smaller pilot injection fuel mass can reduce the soot mass.

77 Although some studies on the use of butanol on engines have been conducted, nowadays the
78 mechanisms that influence the pilot injection and the emissions of diesel engines fueled with
79 *n*-butanol-diesel fuel blends remain largely unknown. Besides, compared to conventional combustion

mode, low temperature combustion often adopts large EGR ratio to reduce the in-cylinder temperature, NO_x, and soot emissions simultaneously. However, a largest EGR ratio would deteriorate the combustion, increase the fuel consumption, lower down the combustion efficiency, and increase HC emissions. Compared to diesel fuel, *n*-butanol has a lower cetane number; blending it with diesel may reduce the cetane number of the blend, and prolong the ignition delay period. This may allow the fuels have adequate time to mix with air to reduce in-cylinder temperature. This study aims to investigate the effects of pilot-injection timing and the fuel mass of pilot injection on low temperature combustion and on the performance of combustion and emissions when using *n*-butanol/diesel blends. The study adopts a high speed, four-cylinder, common-rail diesel engine under the operating condition of medium EGR ratio.

2. Experimental setup and methods

2.1 The experimental setup

Figure 1 shows the sketch of the experimental apparatus, while Table 1 summarizes the technical specifications of test engine. The test system consisted of an engine, a dynamometer and its controller, a fuel supply system (including a fuel tank, a fuel filter, a fuel consumption monitor, a fuel pump and pipe lines); a data acquisition unit, an EGR unit, an exhaust gas analyzer and a smoke meter, sensors dedicated to the measurement of crank angle, temperatures, and in cylinder pressure.

Table 1

Technical specification of test engine

Model	specification
Number of cylinders	4
Cylinder diameter (mm)	85
Number of valves	16
Stroke (mm)	88.1
Displacement (L)	1.99
Maximum torque (Nm)	286
Compression ratio	16.5
Rated Power (kW)/ Speed(r/min)	100/4000

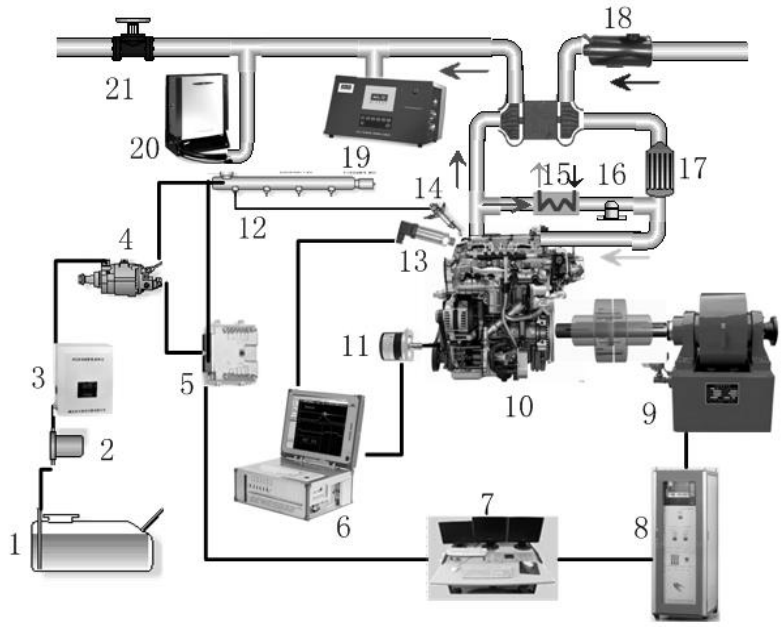

1: Diesel fuel tank; 2:Fuel filter;

3:Fuel consumption monitor; 4:High pressure fuel pump;

5:ECU; 6:Data acquisition;

7:ECU controller; 8:Dyamometer controller;

9: eddy-current dynamometer; 10:Diesel engine;

11:Crank angle sensor; 12:Common-rail;

13:Pressure sensor; 14:Direct injector;

15:Heat exchanger; 16:EGR valve;

17:Heat exchanger; 18:Air filter;

19:Exhaust gas analyzer; 20:Smoke meter;

21:Back pressure valve

Fig. 1 Schematic diagram of the experimental system

The testing engine adopted variable-geometry turbocharger (VGT), EGR, direct-injection, and high-pressure common rail fuel injection system. A measurement, calibration and diagnostic software (INCA, by ETAS) and a Bosch open-type ECU (Engine Control Unit) controlled the common rail fuel injection system. Through ECU, users accommodated parameters like injection fuel mass, injection timing, rail pressure, and pilot injection. Besides, INCA adjusted the opening of EGR valve and nozzle flow area to control the EGR ratio and inlet pressure. A piezoelectric transducer (Kistler 6052CU20) installed on the cylinder head at the position of the glow plug measured the in-cylinder pressure; using these data coming from the piezo-transducer, the rate of heat release and that of pressure rise were calculated. The exhaust emissions from diesel combustion and *n*-butanol-diesel blends fuel combustion were measured and analyzed with a NO_x analyzer (AVL DiGas 4000 Light) and a soot analyzer (AVL Dismoke 4000).

2.2 Experimental fuels

The commercially available 0# diesel fuel, which meets the China Stage III standard for diesel

fuels (equivalent to European III standard), was used as the base fuel. *n*-butanol purchased from local commercial representatives certified to a purity of 99.5% (analytical grade), was chosen as the oxygenated alternative fuel in addition to the base fuel. Blends of 0%, 20%, and 30% by volume fraction of *n*-butanol were tested, expressed as B0, B20, and B30 according to Zheng Chen [30]. B0 represents neat diesel used for all baseline runs; B20, B30 were used to investigate the influence of *n*-butanol ratio (concentration) on combustion performance and emissions of the engine. EGR ratios were set as 0% and 25% respectively. According to author's previous study, as for soot the 25% EGR rate is a turning point before drastic increase. Due to their different fuel properties, the smoke values of the fuels are quite different at 25% EGR rate, as would be explained in detail in following sections.

Table 2 summarizes the properties of diesel and *n*-butanol. The *n*-butanol has higher oxygen concentration and lower cetane number than diesel, so the more the butanol is blended, the higher the oxygen concentration and lower cetane number in the blend.

Table 2

Fuel properties

Fuel properties	Diesel fuel	*n*-Butanol
Density at 20 ºC (g/ml)	0.84	0.81
Cetane number	50-53	~25
Lower calorific value (MJ/kg)	43	33.1
Auto-ignition temperature (ºC)	200-220	385
Boiling point (ºC)	180-230	117.7
Stoichiometric air fuel ratio	15	11.2

Latent heat of evaporation (kJ/kg)	250	585
Flammability limits (% by volume of air)	1.5-7.6	1.4-11.2
Oxygen (% weight)	0	21.6

Properties of diesel and *n*-butanol are from the Ref. [30]

2.3 Experimental tests

Engine performance and exhaust emission tests were performed under the same environmental conditions for each blend. The engine speed was kept at constant speeds of 2000 rpm corresponding to the maximum brake torque conditions. During the engine tests, cooling water temperature was stable at 85±3 °C via PT-100 temperature sensors, the inlet air temperature was 30±2 °C, the inlet air pressure was 0.183 MPa, the main-injection timing of fuel set at -8°CA ATDC (after top dead center), and injection pressure was 120 MPa. The total heat value of each cycle for each fuel was kept constant, which was equal to 30 mg/cycle of diesel according to the lower heating value.

The pilot-injection fuel mass was set at 6 mg. Three different pilot-injection timings (-30 °CA ATDC, -45 °CA ATDC, and -60 °CA ATDC) were designed and tested separately. According to author's previous study, over advanced pilot injection timings result in unacceptable maximum pressure rise rate, while a deteriorated thermal efficiency and unstable combustion always accompanies with an over late injection timing. Therefore, to ensure thermal efficiency and stable operation to the engine, the pilot injection timing was selected within the range (-30 °CA ATDC, -45 °CA ATDC, and -60 °CA ATDC).

The pilot-injection timing was set at -30 °CA ATDC; the total injection mass controlled the total heat value of each cycle for each fuel was kept constant, equal to 30 mg/cycle of diesel according to the lower heating value. Four different pilot-injection masses (2 mg, 4 mg, 6 mg, and 8 mg respectively)

were designed and tested separately. 2 mg was the minimum value of pilot-injection masses in the engine map tested.

The engine operated with either diesel fuel or diesel/n-butanol blends for 10 min to warm up and then tests on engine performance and exhaust emissions parameters with different fuels were carried out according to ISO 8178-6 standard requirements [31]. To avoid the effects of atmospheric humidity and temperature variations, and to ensure measurement precision, experiments were all performed on the same day. To reduce experimental uncertainty and increase the reliability of test results, tests were repeated three times.

Table 3 summarizes the measurements uncertainty Total uncertainty = Square root of {(uncertainty of NOx)^2 + (uncertainty of Soot)^2 +(uncertainty of load)^2 + (uncertainty of speed)^2 + (uncertainty of temperature)^2 + (uncertainty of air flow rate)^2 + (uncertainty of diesel fuel measurement)^2 + (uncertainty of n-butanol measurement)^2 + (uncertainty of pressure pickup)^2 + (uncertainty of crank angle encoder)^2}

= Square root of {$(1)^2 + (0.1)^2 +(0.2)^2 + (0.1)^2 + (0.15)^2 + (1)^2 + (1)^2 + (1)^2 + (0.1)^2 + (0.2)^2$}

= 4.13%.

Table3.

Uncertainties and experimental measurement techniques

Measurement	% Uncertainty	Measurement technique
NOx	±1	Electrochemical measurement
Soot	±0.1	Light transmittance method

Load	±0.2	Strain gauge type load cell
Speed	±0.1	Magnetic pickup principle
Temperature	±0.15	Thermocouple
Air flow rate	±1	Orifice meter
Diesel fuel measurement	±1	Volumetric measurement
N-butanol measurement	±1	Volumetric measurement
Pressure pickup	±0.1	Magnetic pickup principle
Crank angle encoder	±0.2	Magnetic pickup principle

185

186 **2.4 Numeric setup**

187 To better understand the mechanism by which the increase of *n*-butanol ratio prolongs the ignition
188 delay, a zero-dimensional combustion model of engine was established by using chemical kinetics
189 software CHEMKIN. To simulate the combustion of n-butanol-diesel fuel blends, Zhou et al. proposed
190 a simplified reaction mechanism for *n*-heptane-n-butanol-PAHs-toluene mechanism [32]. The
191 parameters of engine simulation are the same as in the experimental engine. All simulations were
192 conducted at engine speed of 2000 rpm, inlet temperature of 300 k, and inlet pressure of 0.183 MPa.

193 **3. Results and discussion**

194 **3.1 Effects of pilot injection timing**

195 Figure 2 shows the results of in-cylinder pressure and heat release using the B20 fuel blend (EGR
196 ratio kept at 25%). The curves show two different peaks for heat release rate corresponding to the pilot
197 injection and to the main injection, respectively. With the increase of pilot injection timing, the peak
198 value of heat release rate in pilot injection reduces when pilot injection timing occurs earlier. In fact,
199 when the piston is far from TDC (top dead center) the volume is larger, and temperature and pressure
200 are lower. The longer ignition delay time promotes the formation of lean and even mixture, which

slows down the heat release rate and lowers the peak value.

The advance of pilot injection timing leads the heat release rate peak value in the main injection ascend slightly because the in-cylinder pressure and temperature are low when fuel is pre-injected. The ignition delay prolongs to form lean and even mixture; the excessively lean mixture delays the combustion of the blends backward to the main injection period, increasing the fuel mass in the combustion related to the main injection, and causing the ascend of heat release rate peak value. However, the heat release of main injection occurred after TDC and the cylinder volume enlarges lowering the combustion temperature; thus, the advance of pilot injection timing, leads to decline the peak value of combustion pressure in main injection period.

When delaying pilot injection time, the higher pressure and temperature in cylinder enable the pre-injected fuel reaching the ignition point quickly. This causes the increase of the pressure in the cylinder, as Figure 2 shows. The in-cylinder pressure for the pilot injection timing at ATDC -30 °CA is higher than that of – 45 °CA and – 60 °CA. Less obviously, the cylinder pressure increases when the pilot injection time delays from -45 °CA to -60 °CA mainly because the lower initial temperature and pressure in cylinder affect the subsequent burning, leading the cylinder pressure increase.

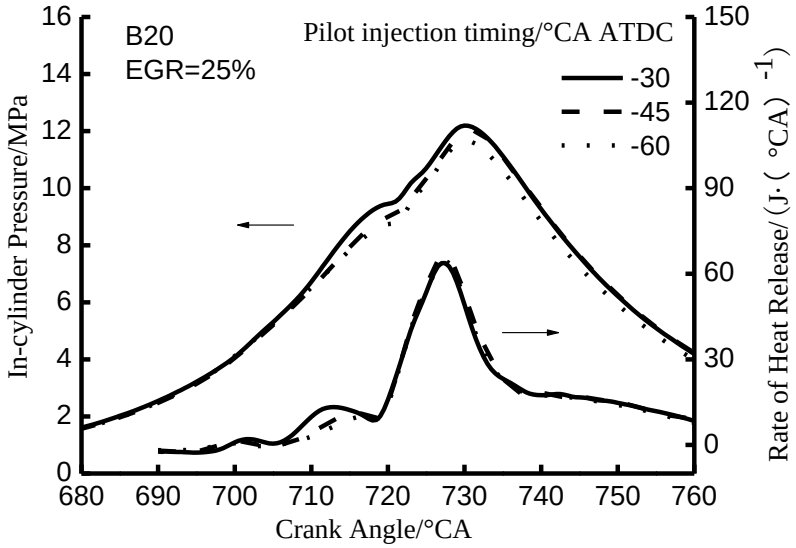

Fig. 2 In-cylinder pressure and heat release rate using B20 for different pilot injection timing

217

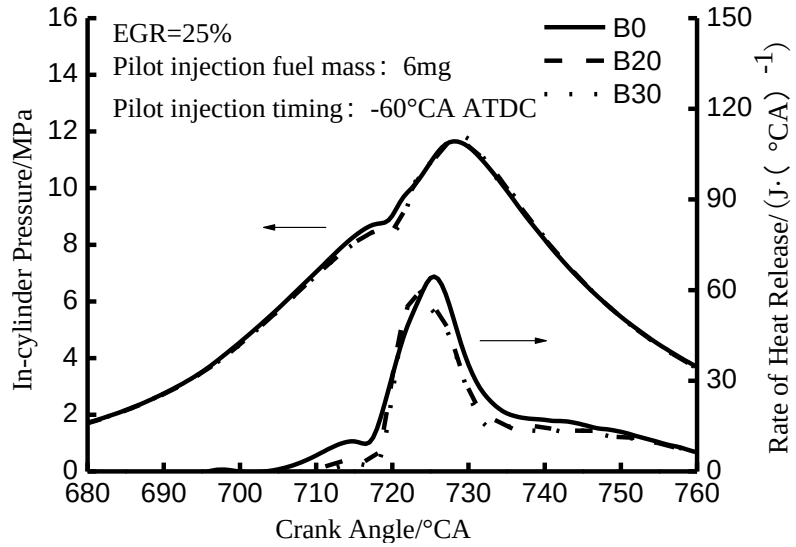

Fig. 3 In-cylinder pressure and heat release rate for different *n*-butanol ratio at EGR 25%

218 Figure 3 shows the in-cylinder pressure and heat release rate using B0, B20, and B30 (settings:
219 EGR ratio 25%,pilot injection fuel mass 6 mg, and pilot injection timing -60 °CA ATDC): with the
220 increase of *n*-butanol ratio, the ignition delay prolongs and heat release timing postpones.

221 To investigate the influence of addition of *n*-butanol on the key chemical reactions that determine
222 the ignition timing, sensitivity analysis of ignition timing for B0 and B20 were conducted at zero EGR

ratios. Fig.4 and Fig.5 were the analysis consequences for key reactions which determined the ignition time. The pictures demonstrated that adding n-butanol, the key reactions nearly were the same for different fuel; however, in the key reaction that took place in B20 blend the dehydrogenation reaction between *n*-butanol and OH free radicals damped the ignition. The dehydrogenation reaction first occurred in *n*-heptane to generate OH free radicals, and the addition of *n*-butanol consumed OH free radicals, which caused n-heptane lack adequate free radicals to have further reactions. Thus, the addition of *n*-butanol hindered the combustion and the ignition time delayed.

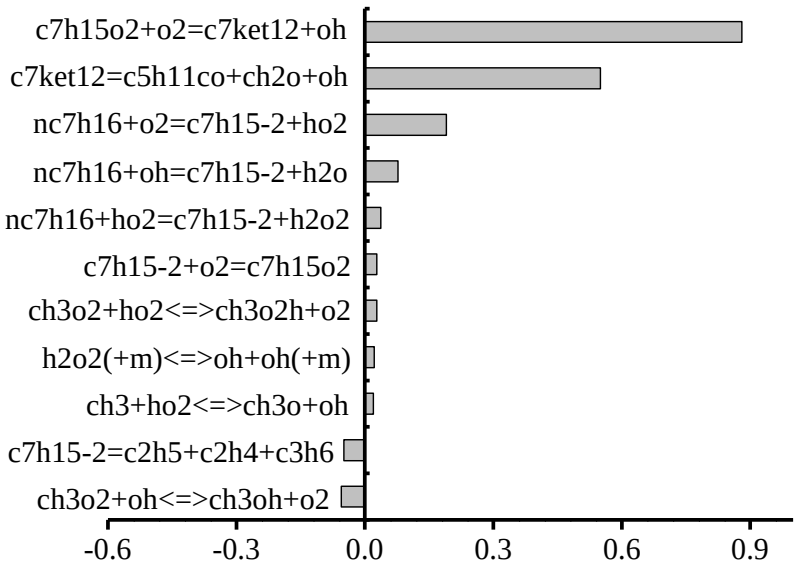

Fig.4 Temperature A-factor sensitivities at the time of ignition for *n*-butanol combustion, B0, EGR0

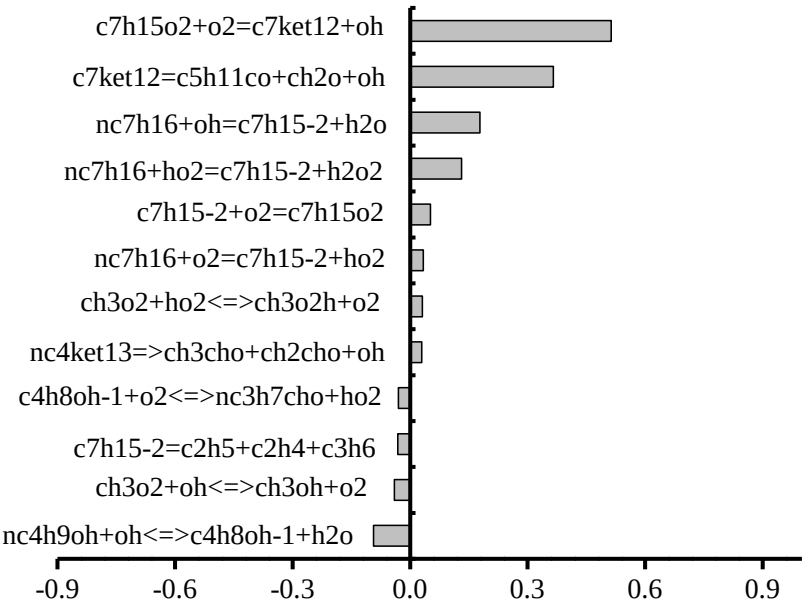

Fig.5 Temperature A-factor sensitivities at the time of ignition for 1-butanol combustion. B20, EGR0

Fig. 6 shows the mole fraction of *n*-heptane consumed through reaction R2 of the total *n*-heptane consumption during the period from the beginning to 20% of fuel quality consumption (zero EGR ratio). The picture shows that the increase of *n*-butanol ratio continuously decreases the fraction of *n*-heptane consumed through the reaction between *n*-heptane and OH. Because the addition of *n*-butanol consumed OH, the quantity of OH that would react with *n*-heptane decreases, the mole fraction decreases by preventing the combustion process and delaying the ignition time.

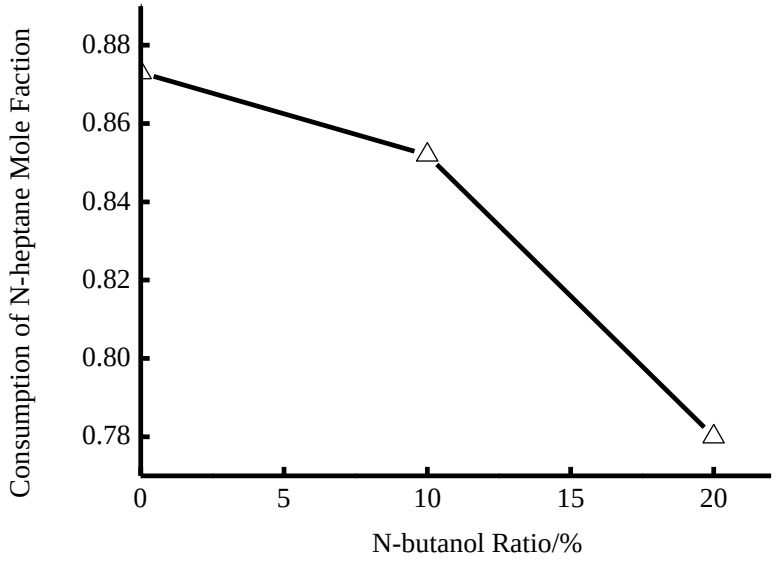

Fig.6 Mole fraction of *n*-heptane consumption

Figure 7 demonstrates the effect of pilot injection timing on maximum pressure rise rate for different *n*-butanol ratios (EGR 25%). The curves show that in all tests the maximum pressure rise rate increases with the advance of pilot injection. In fact, the in-cylinder pressure (see Figure 2) and temperature are lower when fuels are pre-injected and the mixture of fuel and air is too lean to burn. The mixture burns rapidly together with the fuel injected during the main injection period and causes the ascending maximum pressure rise rate.

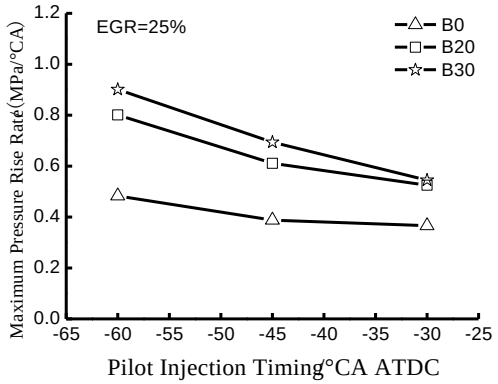

Fig. 7 Effect of pilot injection timing on the maximum pressure rise rate (different *n*-butanol ratio)

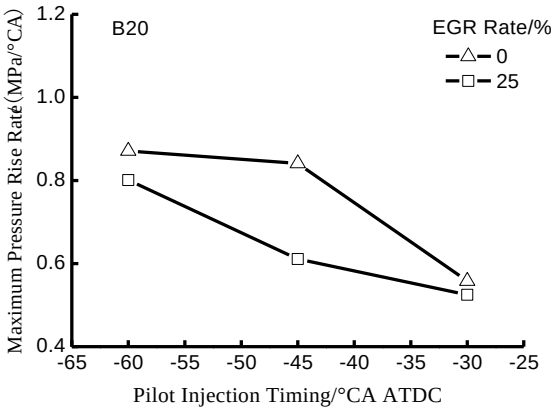

Fig. 8 Effect of pilot injection timing on the maximum pressure rise rate (different EGR rates)

Figure 7 also shows that the maximum pressure rise rate ascends with the increase of *n*-butanol. In fact, with the increase of *n*-butanol, fuel cetane number and lower calorific value decrease. Moreover, extending ignition delay allows more combustible mixture generate. The mixture burns rapidly with the fuel in the main injection period, causing the maximum pressure rise rate ascending.

Figure 8 shows the effect of pilot injection timing on the maximum pressure rise rate in the main injection period using B20 at different EGR rates. The curves show that the maximum pressure rise rate decreases with the increasing of EGR ratios. Thus, EGR reduces the maximum pressure rise rate. In fact, the introduction of EGR prolongs the ignition delay by reducing the oxygen concentration in

cylinder. Due to EGR, the specific heat increases, the main combustion rate slows down and the maximum pressure rise rate reduces, softening the combustion.

Figure 9 shows the effects of pilot injection timing on brake specific fuel consumption (BSFC) at different *n*-butanol ratios at EGR ratio 25%, while Figure 10 shows the same effects using B20 at different EGR ratios.

Curves highlight that the advance of pilot injection timing leads to BSFC increasing; moreover, the brake thermal efficiency decreases because the heat release of pilot injection occurs far away from TDC, increasing heat transfer loss, frictional loss, and negative compression work of air/fuel mixture. These changes decrease brake thermal efficiency, thus BSFC increase.

Figure 12 also shows how the brake specific fuel consumption ascends with the increase of *n*-butanol ratios: *n*-butanol has a LHV (Low heating value) smaller than diesel, and the increase of *n*-butanol ratios and constant injection fuel mass per cycle cause the total heat release decrease. Thus, output work reduces, the brake thermal efficiency descends, and the BSFC ascends, as shown in Figure 11 and 12.

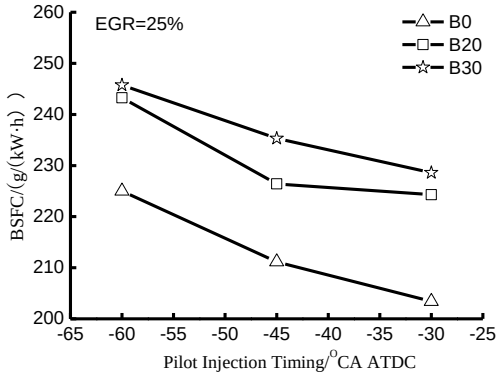

Fig. 9 Effect of pilot injection timing on BSFC at different *n*-butanol ratio

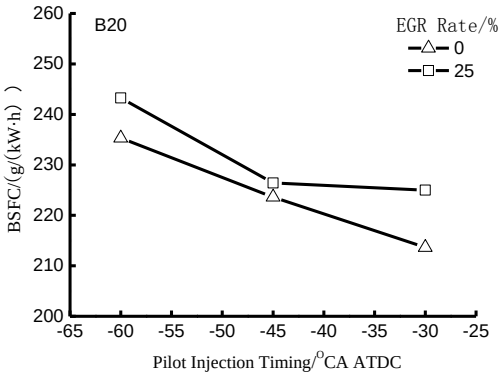

Fig. 10 Effect of pilot injection timing on BSFC at different EGR rate

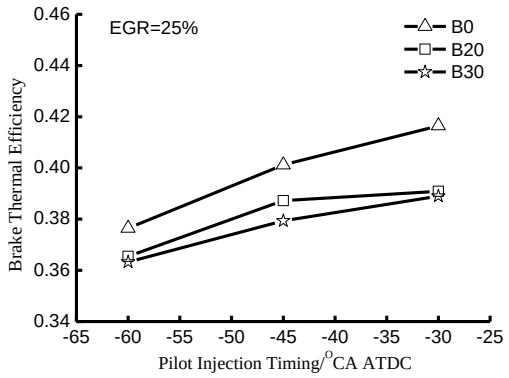

Fig. 11 Effect of pilot injection timing on brake thermal efficiency at different *n*-butanol ratio

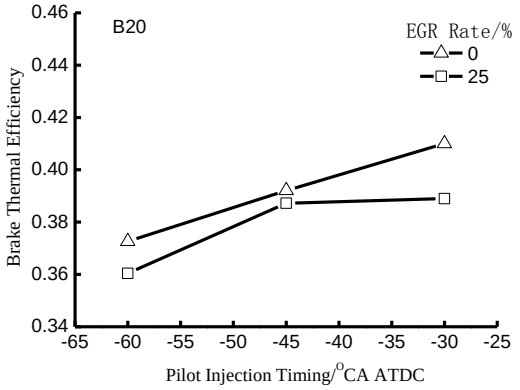

Fig. 12 Effect of pilot injection timing on brake thermal efficiency at different EGR rate

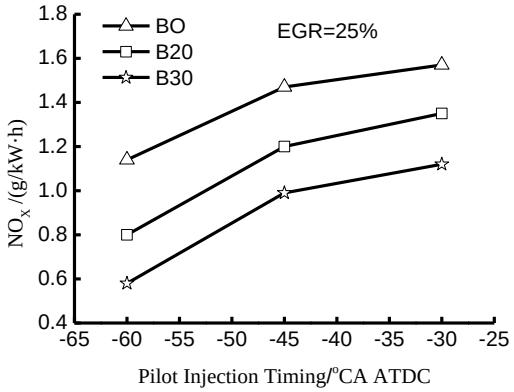

Fig. 13 Effect of pilot injection timing on NO_x emission at different *n*-butanol ratio

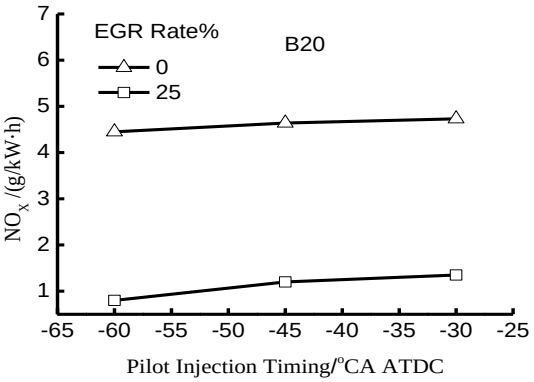

Fig. 14 Effect of pilot injection timing on NO_x emission at different EGR rate

Figures 10 and 12 show that with the increase of EGR ratio the brake specific fuel consumption increases and the brake thermal efficiency decreases since the introduction of EGR dilutes the mixture lowering the combustion temperature.

To take the humidity effect on NO_x formation into account, a dimensionless correction factor was calculated as [33]:

$$k_{h,D} = \frac{1}{1-0.0182\times(H_a-10.71)+0.045\times(T_a-289)} \quad (1)$$

where H_a humidity of the intake air (g H_2O/kg dry air) and T_a temperature of the intake air (K). H_a and T_a were measured by AR807 with an accuracy of ±5 RH% and ±1 °C. The concentration values of NO_x emissions are converted into mass values using the following relationship:

$$NO_X(mass) = 0.001587 \times [NO_X]_{wet} \times k_{h,D} \times G_{EXHW} \quad (2)$$

where NO_x(mass) is the corrected emission concentration (g/h), $[NO_x]_{wet}$, is the emission concentration on a wet basis (ppm) and G_{EXHW} are the exhaust gas average molecular weights (g/h) [33,34]. The emission results were expressed on brake specific (g/kW h) basis for each test case examined in below.

Figure 13 shows the effect of pilot injection timing on NO_x emission at different *n*-butanol ratios, with EGR ratio as 25%. Figure 14 shows the same effects using B20 at different EGR ratios. Figures 13 and 14 show that advancing pilot injection timing allows NO_x emission decrease. It is well known NO_x strongly depends on in-cylinder temperature [35,36]. The in-cylinder pressure and temperature are lower when fuel is pre-injected; the ignition delay prolongs to form the excessively leaner air/fuel mixture, then the combustion temperature reduces, and NO_x emissions reduce.

Figure 13 also shows that with the increase of *n*-butanol ratio, NO_x emissions decrease because the increasing of *n*-butanol ratio prolongs the ignition delay and fuel has adequate time to mix with air to form a leaner and even mixture. In addition, the LHV of *n*-butanol is lower than diesel fuel, causing lower combustion temperature and lower NO_x formation and emissions. Figure 14 shows that with the increase of EGR ratio, the NO_x emission decreases mainly because the introduction of EGR reduces the oxygen concentration, increasing the specific heat and lowering the combustion temperature, which reduce NO_x formation and emission.

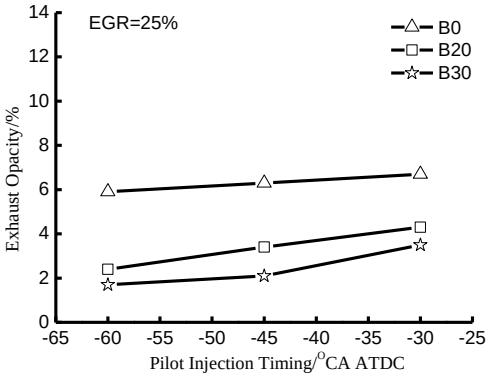

Fig. 15 Effect of pilot injection timing on soot emission (different *n*-butanol ratio)

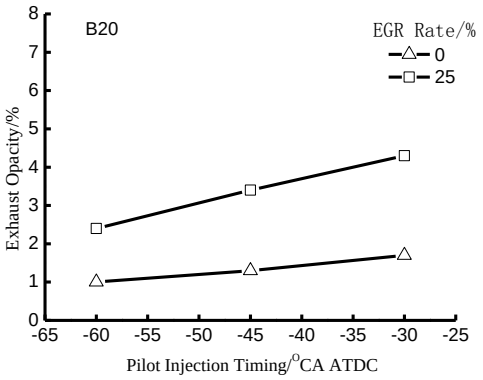

Fig. 16 Effect of pilot injection timing on soot emission (different EGR rate)

Figure 15 shows the effect of pilot injection timing on soot emission at different *n*-butanol ratios and EGR ratio 25%. The curves show that the soot emission decreases with the advance of pilot injection timing because it ensures the fuel having adequate time to blend with the air in cylinder to form even combustible mixture; the combustion processes more thoroughly and the soot emission decreases. Figure 15 also demonstrates that the increase of *n*-butanol ratio reduces soot emissions because the long ignition delay period of *n*-butanol ensures an adequate mixture between fuel and air. Besides, the oxidation of oxygen atom of *n*-butanol can reduce the generation of soot.

Figure 16 shows the effect of pilot injection timing on soot emissions for B20 at different EGR ratios. The figure shows that the introduction of a medium EGR ratio causes soot emissions ascending because the addition of EGR lowers combustion temperature leading to the incomplete combustion. Moreover, the high specific heat of EGR lowers the combustion temperature, which has a negative effect on soot oxidation. Besides, when the pilot injection timing delays, the main-injected fuel comes into the combustion process of pilot injection fuel and causes oxygen deficiency, increasing the soot emission.

Table 4 compares different engine performances fueled with B20 and with B0 fixing the pilot-injection timing at -30 °CA ATDC, the pilot injection mass at 6 mg.

Table 4

Relative engine performances under different pilot-injection timing

Pilot injection Timing (°CA ATDC)	Relative BSFC (%)	Relative brake thermal efficiency (%)	Relative NO_x(%)	Relative soot (%)
-30	+10.3%	-6.1%	-14.0%	-35.8%
-45	+11.3%	-7.0%	-23.6%	-49.3%
-60	+20.0%	-12.2%	-49.0%	-64.2%

The more advanced the pilot-injection timing, the less the emissions of NO_x and soot; however, BSFC increased and thermal efficiency decreased.

3.2 Effect of the fuel mass on pilot injection

Figure 17 and Figure 18 show the combustion performance for different fuel mass of pilot injection using different *n*-butanol ratios when EGR is set to 0 and to 25%: increasing the fuel mass pilot injection, two stages of heat release occur. The first stage takes place in pre-injected fuel, while the second stage in main-injected fuel wherein the instant heat release peak-value descends and combustion pressure peak value ascends. The trend refers to the increase of pilot injection fuel mass, when more heat is released causing the instant heat release peak-value for pre-injected fuel arise. As the pilot injection fuel mass increases, the main-injected fuel mass reduces when the total amount of the fuel injection is fixed. Thus, the instant heat release peak-value for main injected fuel descends. In

334 addition, the higher heat release from pre-injected fuel leads to pressure and combustion chamber

335 temperature increase, and the main injected fuel intensifies the combustion process.

336

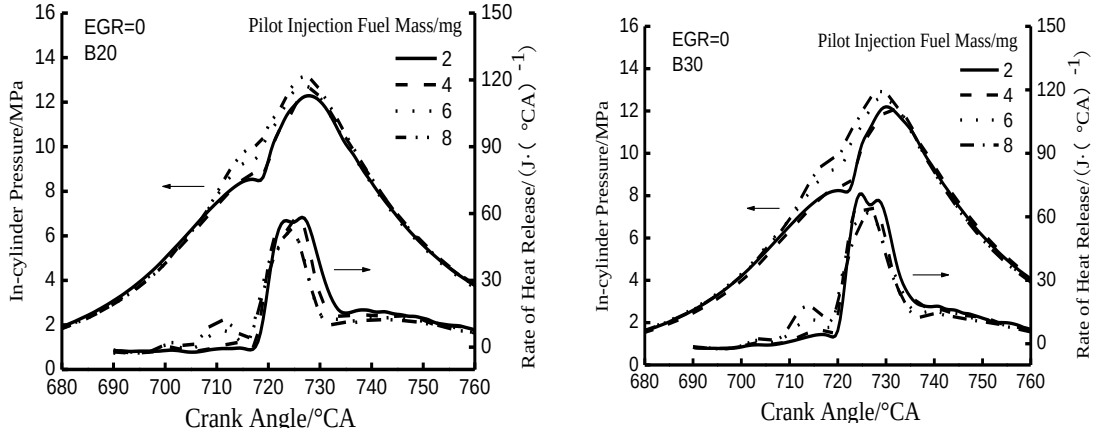

(a) B20, effect of pilot injection mass on in-cylinder pressure and heat release rate

(b) B30, effect of pilot injection mass on in-cylinder pressure and heat release rate

Fig. 17 Combustion performance for different pilot injection fuel mass at different *n*-butanol ratio (EGR = 0)

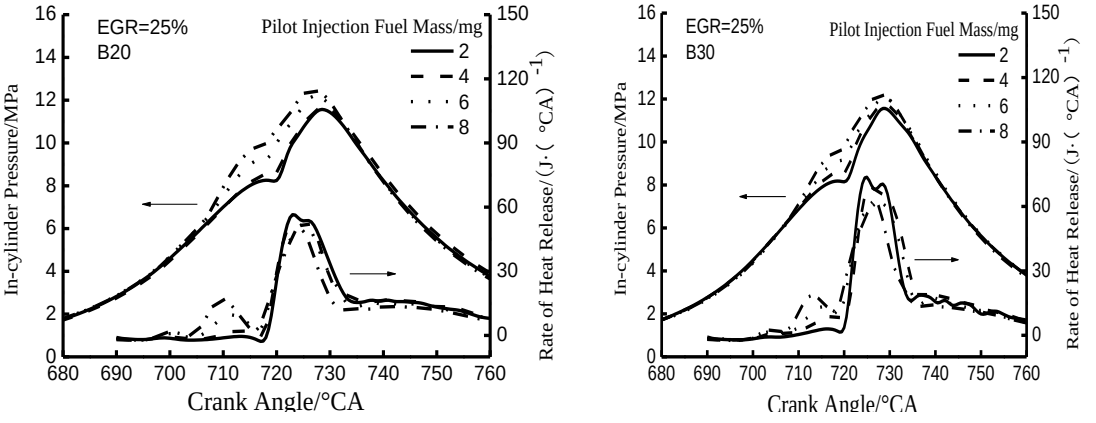

(a) B20, the effect of pilot injection mass on in-cylinder pressure and heat release rate

(b) B30, the effect of pilot injection mass on in-cylinder pressure and heat release rate

Fig. 18 Combustion performance for different pilot injection fuel mass at different *n*-butanol ratio

(EGR=25%)

Figure 19 shows the effect of pilot injection fuel mass on CA50 (for a single cylinder CA50 is defined as the crank angle corresponding to 50% of the maximum apparent heat release) at different *n*-butanol ratios, when EGR ratio is 25%. The curves show that with the increase of pilot injection fuel mass, CA50 advances because the higher heat released and the ignition delay of main injection fuel shortened. Therefore, the heat release rate of main injection phase is faster, and advances the CA50. Figure 19 also shows that CA50 advances with the increase of *n*-butanol ratio because lower cetane number of *n*-butanol prolongs the ignition delay. Thus, the extension increases the pre-mixture of air/fuel, and oxygen atoms of *n*-butanol promote fuel oxidation to release heat. Besides, the higher volatility of *n*-butanol mixes it with air quickly to form additional air/fuel mixture.

Figure 20 shows the effects of pilot injection fuel mass on CA50 at different EGR rates using B20: with the increase of EGR, CA50 postponed And EGR reduces the mixture oxygen concentrations. Then, combustion rate slows down and temperature decreases, delaying the CA50.

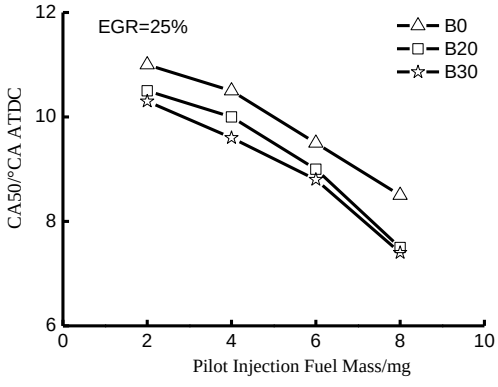

Fig. 19 Effect of pilot injection fuel mass on CA50 at different *n*-butanol ratios

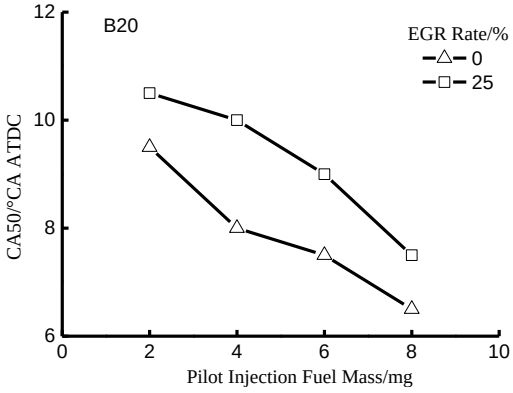

Fig. 20 Effect of pilot injection fuel mass on CA50 at different EGR rate

Figure 21 and Figure 22 show the effects of pilot injection fuel mass on brake specific fuel consumption and brake thermal efficiency at different *n*-butanol ratios; in both cases, EGR ratio is set at 25%. Figure 21 highlights that increasing pilot injection fuel mass increases brake specific fuel consumption because the pre-injected fuel burns far away from TDC, thus the negative compression work increases and lowers down the brake thermal efficiency.

Figure 21 also shows that increasing the *n*-butanol ratio while keeping the total injection fuel mass constant causes the brake specific fuel consumption increase. In fact, *n*-butanol has a lower Lower calorific value than diesel. Increasing of *n*-butanol ratio and keeping the total injection fuel mass constant, the total heat release of mixture decreases reducing the effective power. Thus, the brake thermal efficiency decreases and brake specific fuel consumption increases.

Figure 23 and Figure 24 shows the effect of pilot injection fuel mass on brake specific fuel consumption and brake thermal efficiency using B20 with different EGR rates. Figure 23 also shows that with the increase of pilot injection fuel mass, brake specific fuel consumption increases. Moreover, the figure shows how the EGR rate increases increasing the brake specific fuel consumption because the introduction of EGR reduces the oxygen concentration, making the combustion process incomplete.

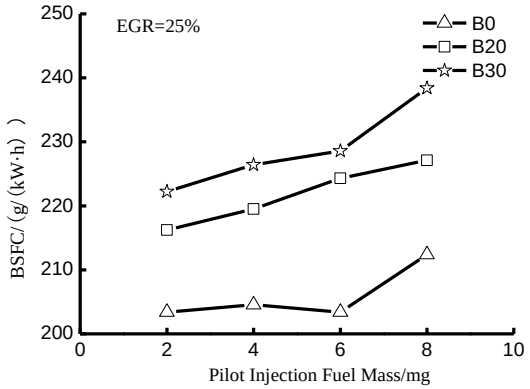

Fig. 21 Effect of pilot injection fuel mass on BSFC at different *n*-butanol ratios

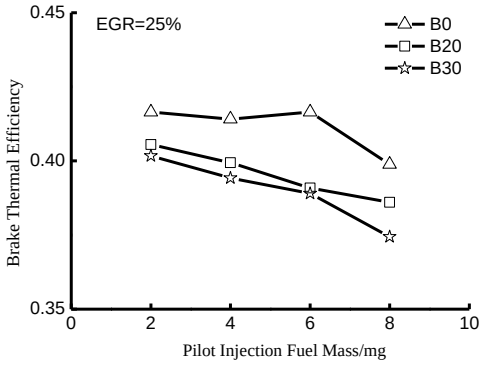

Fig. 22 Effect of pilot injection fuel mass on brake thermal efficiency at different *n*-butanol

ratios

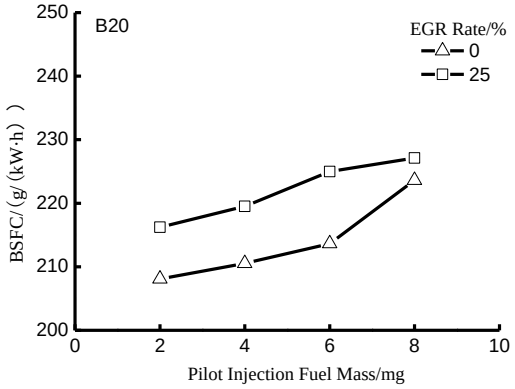

Fig. 23 Effect of pilot injection fuel mass on BSFC at different EGR rate

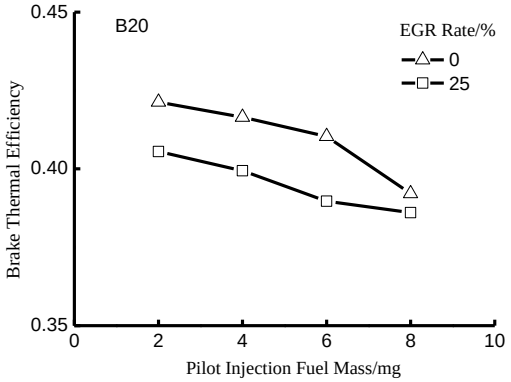

Fig. 24 Effect of pilot injection fuel mass on brake thermal efficiency at different EGR rate

Figure 25 shows the effect of pilot injection fuel mass on NO_x emissions at different *n*-butanol ratios when EGR rate is 25%, while Figure 26 shows the same effects using B20 with different EGR rates. The figures show that with the increase of pilot injection fuel mass, NO_x emissions increase because increasing the pilot injection fuel mass causes the air/fuel mixture in cylinder increase, and the temperature of the gases increases when the main injection fuel burns. The higher temperature in cylinder increases NO_x emissions.

Figure 25 also shows that increasing *n*-butanol ratio NO_x emissions decrease because the increasing of *n*-butanol ratio prolongs the ignition delay, giving fuel an adequate time to blend with air to form leaner and even mixture. In addition, the heating value of *n*-butanol is lower than diesel, thus combustion temperature is lower, and NO_x formation and emissions reduces.

Figure 26 demonstrates that the NO_x emissions decrease with the increase of EGR rate because increasing the EGR reduces the fresh air concentration and dilutes the air/fuel mixture. The combustion

rate slows down and the decrease of combustion temperature causes the reduction of NO_x emissions.

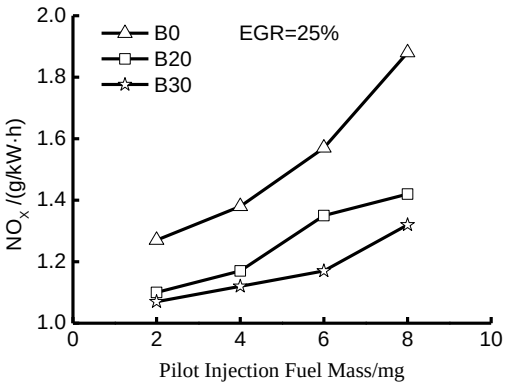

Fig. 25 Effect of pilot injection fuel mass on NO_x emission at different *n*-butanol ratios

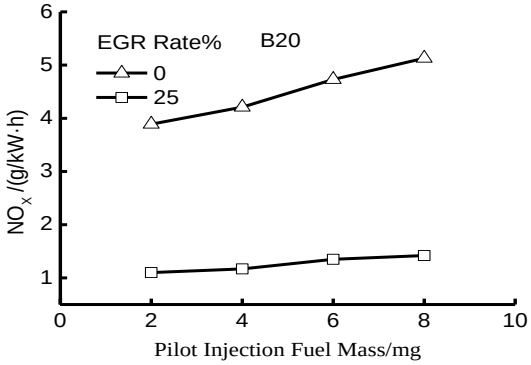

Fig. 26 Effect of pilot injection fuel mass on NO_x emission at different EGR rate

Figure 27 shows the effect of pilot injection fuel mass on soot emissions at different *n*-butanol ratios when EGR rate was 25%, while Figure 28 shows the same effects using B20 at different EGR rates. Increasing the pilot injection fuel mass causes soot emissions decreasing at first. Then, they increase because the increase of pilot injection fuel mass promotes the evaporation and atomization of the main-injected fuel to form the even mixture, promoting soot emissions reduction.

In addition, the increase of pilot injection fuel promotes the formation of air/fuel pre-mixture. The main-injected fuel mass decreases and shortens the diffusive combustion stage. Since the soot generation process is mainly concentrated during the diffusive combustion stage, increasing the pilot injection fuel would reduce the soot emission. However, when pilot injection fuel increases further, the heat release increased further too shortening the main injection ignition delay. Thus, the mixing time for fuel and air also reduces and the mixture of air/fuel uneven, increasing soot emissions. Besides, when pilot injection fuel mass increases, the collision of atoms with walls takes place and this part of fuel evaporated too slowly to mix with air. The local formation of an excessive fuel-rich area avoids the

complete fuel combustion and increases soot emissions.

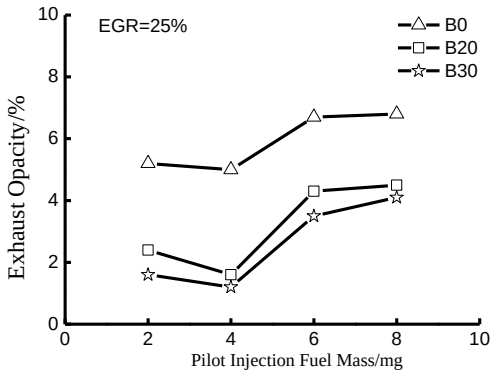

Fig. 27 Effect of pilot injection fuel mass on soot emission at different *n*-butanol ratios

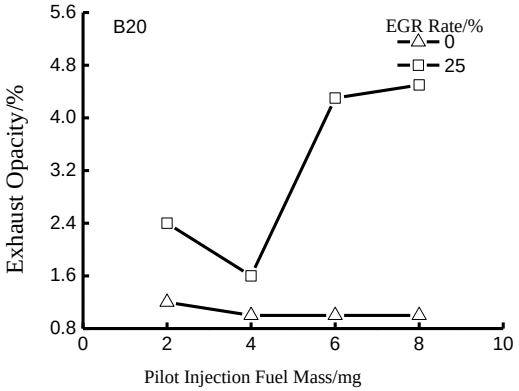

Fig. 28 Effect of pilot injection fuel mass on soot emission at different EGR rate

Figure 27 also demonstrates that with the increase of *n*-butanol ratio, soot emissions decrease because the increase of *n*-butanol ratio prolongs the ignition delay, and fuel adequately blends with air reducing the local excessively fuel rich area and soot emissions. Besides, the *n*-butanol oxygen atoms oxidize soot decreasing further soot emissions. Figure 28 shows that a 25% EGR rate increases soot emissions because the addition of a certain amount of EGR decreases oxygen concentration causing the incomplete combustion. Moreover, the EGR higher specific heat capacity may decrease the combustion temperature and decreases further soot oxidation.

Table 5 compares engine performances in terms of relative differences considering an engine fueled with B20 compared to B0 fixing pilot-injection timing at -30 °CA ATDC, and pilot injection mass at 6 mg.

Table 5

Engine performances: comparison between B20 with B0 under different pilot-injection fuel mass

Pilot injection fuel mass (mg)	Relative BSFC (%)	Relative brake thermal efficiency (%)	Relative NO_x (%)	Relative soot (%)
2	+6.3%	-2.6%	-29.9%	-64.2%
4	+7.9%	-4.1%	-25.5%	-76.1%
6	+10.3%	-6.1%	-14.0%	-35.8%
8	+11.7%	-7.3%	-9.8%	-32.8%

The table shows that when the pilot-injection mass of B20 fuel increases from 2 to 8, the BSFC increases gradually from 6.3% to 11.7% and the brake thermal efficiency decreases from 2.6% to 7.3%, the emissions of NO_x reduce by 29.9%, 25.5%, 14.0% and 9.8% respectively, while soot reduces by 64.2%, 76.1%, 35.8% and 32.8% respectively. The table shows that when B20 fuel mass is 4 mg, a strong reduction of emissions of NO_x and soot occurs, which does not affect BSFC and the thermal efficiency.

4. Conclusions

In this study, engine performance, combustion and exhaust emissions of turbocharged direct injection diesel engine were evaluated using n-butanol-diesel blends in low temperature combustion at medium EGR ratio; engine speed was constant at 2000 rpm and various pilot injection timing and pilot injection mass investigated. Effects of n-butanol properties of blends, and the effects of pilot injection

timing and pilot injection mass on engine performance and exhaust emissions were discussed in detail. The main conclusions can be drawn:

- Addition of n-butanol to diesel leads to increase the maximum pressure rise rate and BSFC, advance CA50, while decrease NO_x and soot emissions.
- The use of EGR delays CA50, increases BSFC and soot emissions, decreases NO_x emissions.
- Advancing the pilot injection timing decreases the heat release rate peak value of the pre-injected fuel, increases the peak value of heat release rate of the main-injected fuel slightly, decreases the combustion pressure peak value in the main injection period, increases the maximum pressure rise rate and BSFC while it decreases NO_x and soot emissions.
- The more advanced the pilot-injection timing, the less NO_x and soot emissions and thermal efficiency, while the more increasing BSFC.
- Increasing the pilot injection fuel mass increases the heat release peak value of pre-injected fuel, decreases the heat release peak value of main-injected fuel, increases the combustion pressure peak value, the BSFC and NOx emission, while soot emission decreases at first and then increases.
- When the injection mass of B20 is 4 mg, there is a strong reduction of emissions of NOx and soot, which affect little engine BSFC and its thermal efficiency.

Acknowledgement

The research is sponsored by projects of Natural Science Foundation of China (Grant No.51076033), and Natural Science Foundation of Guangxi (project Outstanding Young Scholarship Award, Grant No.2014GXNSFGA118005). This research is financially supported by the project of

outstanding young teachers' training in higher education institutions of Guangxi. This research outcome is also partly from a joint UK–China research project in Bio-fuel Micro-Tri generation with Cryogenic Energy Storage System funded by the Engineering and Physical Sciences Research Council of the UK.

References

[1] Han S, Kim J, Bae C. Effect of air–fuel mixing quality on characteristics of conventional and low temperature diesel combustion. Appl Energy 2014; 119: 454-66.

[2] Shuai S, Abani N, Yoshikawa T, et a1. Evaluation of the effects of injection timing and rate-shape on diesel low temperature combustin using advanced CFD modeling. Fuel 2009;88:1235-44.

[3] Feng H, Zheng Z, Yao M et a1. Effects of exhaust gas recirculation on low temperature combustion using wide distillation range diesel. Energy 2013;51: 291-96.

[4] Han M. The effects of synthetically designed diesel fuel properties-cetane number, aromatic content, distillation temperature, on low-temperature diesel combustion. Fuel 2013;109: 512-19.

[5] Ujor V, Bharathidasan AK, Cornish K, Ezeji TC. Feasibility of producing butanol from industrial starchy food wastes. Appl Energy 2014;136:590-98.

[6] Srirangan K, Akawi L, Young MM, Perry Chou CP. Towards sustainable production of clean energy carriers from biomass resources. Appl Energy 2012;100:172-86.

[7] Ranjan A, Khanna S, Moholkar VS. Feasibility of rice straw as alternate substrate for biobutanol production. Appl Energy 2013;103:32-38.

[8] Zhang ZH, Balasubramanian R. Influence of butanol addition to diesel–biodiesel blend on engine performance and particulate emissions of a stationary diesel engine. Appl Energy

2014;119:530-36.

[9] Irimescu A. Performance and fuel conversion efficiency of a spark ignition engine fueled with iso-butanol. Appl Energy 2012;96:477-83.

[10] Mendez CJ, Parthasarathy RN, Gollahalli SR. Performance and emission characteristics of butanol/Jet A blends in a gas turbine engine. Appl Energy 2014;118:135-40.

[11] Bora P, Konwar LJ, Boro J, Phukan MM, Deka D, Konwar BK. Hybrid biofuels from non-edible oils: A comparative standpoint with corresponding biodiesel. Appl Energy 2014;135:450-60.

[12] Atmanl A, İleri E, Yüksel B. Experimental investigation of engine performance and exhaust emissions of a diesel engine fueled with diesel-n-butanol-vegetable oil blends. Energy Conversion and Management 2014;81:312-21.

[13] Sahin Z, Durgun O, Aksu ON. Experimental investigation of n-butanol/diesel fuel blends and n-butanol fumigation - Evaluation of engine performance, exhaust emissions, heat release and flammability analysis. Energy Conversion and Management 2015;103: 778-89.

[14] Atmanl A, İleri E, Yüksel, B. Karaoglan AD. Response surface methodology based optimization of diesel-n-butanol -cotton oil ternary blend ratios to improve engine performance and exhaust emission characteristics, Energy Conversion and Management 2015;90:383-94.

[15] Zannis TC, Hountalas DT, Kouremenos DA. Experimental investigation to specify the effect of oxygenated addition content and type on DI diesel engine performance and emissions. SAE Technical Paper 2004-01-0097,2004.

[16] Valentino G, Felice E. Corcione, Stefano E. Iannuzzi, Simone Serra. Experimental Study on Performance and Emissions of a High Speed Diesel Engine Fuelled with N-butanol Diesel Blends under Premixed Low Temperature Combustion. Fuel 2012;92: 295-307.

492 [17] Sahin Z, Aksu ON. Experimental investigation of the effects of using low ration-butanol/diesel
493 fuel blends on engine performance and exhaust emissions in a turbocharged DI diesel engine.
494 Renew Energy 2015;77:279-290.
495 [18] Rakopoulos DC, Rakopoulos CD, Giakoumis EG, Dimaratos AM, Kyritsis DC. Effects of
496 butanol–diesel fuel blends on the performance and emissions of a high-speed DI diesel engine.
497 Energy Convers Manage 2010;51:1989-1990.
498 [19] Chen Z, Wu ZK, Liu JP, Lee C. Combustion and emissions characteristics of high n-butanol/diesel
499 ratio blend in a heavy-duty diesel engine and EGR impact. Energy Convers Manage
500 2014;78:787-795.
501 [20] Siwale L, Kristóf L, Adam T, Bereczky A, Mbarawa M, Penninger A, Kolesnikov A. Combustion
502 and emission characteristics of n-butanol/diesel fuel blend in a turbo-charged compression
503 ignition engine. Fuel 2013;107:409-18.
504 [21] Rakopoulos DC, Rakopoulos CD, Hountalas DT, Kakaras EC, Giakoumis EG, Papagiannakis RG.
505 Investigation of the performance and emissions of bus engine operating on butanol/diesel fuel
506 blends. Fuel 2010;89: 2781-90.
507 [22] Oğuzhan Doğan, The influence of n-butanol/diesel fuel blends utilization on a small diesel engine
508 performance and emissions, Fuel, Volume 90, Issue 7, July 2011, Pages 2467-2472
509 [23] Zheng ZQ, Yue L, Liu HF, Zhu YX, Zhong XF, Yao MF. Effect of two-stage injection on
510 combustion and emissions under high EGR rate on a diesel engine by fueling blends of
511 diesel/gasoline, diesel/n-butanol, diesel/gasoline/n-butanol and pure diesel. Energy Convers
512 Manage 2015;90:1-11.
513 [24] Badami M, Mallamo F, Millo F, Rossi EE. Influence of multiple injection strategies on emissions,

514 combustion noise and BSFC of a DI common rail diesel engine. SAE Tech Paper 2002; SAE
515 2002-01-0503.
516 [25] Payri F, Benajes J, Molina S, Riesco JM. Reduction of Pollutant emissions in a HD diesel engine
517 by adjustment of injection parameters, boost pressure and EGR.SAE Tech Paper 2003; SAE
518 2003-01-0343.
519 [26] Hotta Y, Inayoshi M, Nakakita K, Fujiwara K, Sakata I. Achieving lower exhaust emissions and
520 better performance in an HSDI diesel engine with multiple injections. SAE Tech Paper 2005; SAE
521 2005-01-0928.
522 [27] Cheolwoong P, Sanghoon K, Choongsik B. Effects of multiple injections in a HSDI diesel engine
523 equipped with common rail injection system. SAE Tech Paper 2004; SAE 2004-01-0127.
524 [28] Beatrice C, Belardini P, Bertoli C, Del Giacomo N. Downsizing of common rail D.I. engines:
525 influence of different injection strategies on combustion evolution. SAE Tech Paper 2003; SAE
526 2003-01-1784.
527 [29] Thurnheer T, Edenhauser D, Soltic P, Schreiber D, Kirchen P, Sankowski A. Experimental
528 investigation on different injection strategies in a heavy-duty diesel engine: Emissions and loss
529 analysis. Energy Convers Manage 2011;52:457-67.
530 [30] Chen Z, Liu JP, Han ZY, Du B, Liu Y, Lee CF. Study on performance and emissions of a
531 passenger-car diesel engine fueled with butanol-diesel blends. Energy 2013;55:638-646.
532 [31] EN ISO 8178-6. Reciprocating internal combustion engines-exhaust emission measurement-Part 6:
533 Report of measuring results and test. European Committee for Standardization, Brussels, Belgium;
534 2000.
535 [32] Zhou X, Song M, Huang H, Yang R, Wang M, and Sheng J. Numerical study of the formation of

soot precursors during low-temperature combustion of a n-butanol–diesel blend. Energy & Fuels, 2014, 28 (11): 7149-7158.

[33] Directive 2005/55/EC of the European Parliament and of the Council of 28 September; 2005.

[34] d'Ambrosio S, Finesso R, Spessa E. Calculation of mass emissions, oxygen mass fraction and thermal capacity of the inducted charge in SI and diesel engines from exhaust and intake gas analysis. Fuel 2011;90:152–66.

[35] K. Varatharajan, M. Cheralathan. Influence of fuel properties and composition on NOx emissons from biodiesel powered diesel engines: a review, Renew. Sustain. Energy Rev. 16 (2012) 3702-3710.

[36] S.C. Hill, L.D. Smoot. Modeling of nitrogen oxides formation and destruction in combustion systems, Prog. Energy Combust. Sci. 26 (2000) 417-458.

Table captions:

Table 1 Technical specification of test engine.

Table 2 Fuel properties.

Table 3 Uncertainties and experimental measurement techniques.

Table 4 Relative engine performances under different pilot-injection timing.

Table 5 Engine performances: comparison between B20 with B0 under different pilot-injection fuel mass.

Figure captions:

Fig. 1 Schematic diagram of the experimental system.

Fig. 2 In-cylinder pressure and heat release rate using B20 for different pilot injection timing.

Fig. 3 In-cylinder pressure and heat release rate for different *n*-butanol ratio at EGR 25%.

Fig.4 Temperature A-factor sensitivities at the time of ignition for n-butanol combustion, B0, EGR0.

Fig.5 Temperature A-factor sensitivities at the time of ignition for 1-butanol combustion,B20, EGR0.

Fig.6 Mole fraction of *n*-heptane consumption.

Fig. 7 Effect of pilot injection timing on the maximum pressure rise rate (different n-butanol ratio).

Fig. 8 Effect of pilot injection timing on the maximum pressure rise rate (different EGR rates).

Fig. 9 Effect of pilot injection timing on BSFC at different *n*-butanol ratio.

Fig. 10 Effect of pilot injection timing on BSFC at different EGR rate.

Fig. 11 Effect of pilot injection timing on brake thermal efficiency at different n-butanol ratio.

Fig. 12 Effect of pilot injection timing on brake thermal efficiency at different EGR rate.

Fig. 13 Effect of pilot injection timing on NOx emission at different n-butanol ratio.

570 Fig. 14 Effect of pilot injection timing on NOx emission at different EGR rate.

571 Fig. 15 Effect of pilot injection timing on soot emission (different n-butanol ratio).

572 Fig. 16 Effect of pilot injection timing on soot emission (different EGR rate).

573 Fig. 17 Combustion performance for different pilot injection fuel mass at different n-butanol ratio
574 (EGR = 0).

575 Fig. 18 Combustion performance for different pilot injection fuel mass at different n-butanol ratio
576 (EGR=25%).

577 Fig. 19 Effect of pilot injection fuel mass on CA50 at different n-butanol ratios.

578 Fig. 20 Effect of pilot injection fuel mass on CA50 at different EGR rate.

579 Fig. 21 Effect of pilot injection fuel mass on BSFC at different n-butanol ratios.

580 Fig. 22 Effect of pilot injection fuel mass on brake thermal efficiency at different n-butanol ratios.

581 Fig. 23 Effect of pilot injection fuel mass on BSFC at different EGR rate.

582 Fig. 24 Effect of pilot injection fuel mass on brake thermal efficiency at different EGR rate.

583 Fig. 25 Effect of pilot injection fuel mass on NOx emission at different n-butanol ratios.

584 Fig. 26 Effect of pilot injection fuel mass on NOx emission at different EGR rate.

585 Fig. 27 Effect of pilot injection fuel mass on soot emission at different n-butanol ratios.

586 Fig. 28 Effect of pilot injection fuel mass on soot emission at different EGR rate.